 FDMP, vol.10, no.3, pp.377-393, 2014

Numerical Study of Combined Natural Convection-surface Radiation in a Square Cavity

S. Hamimid[1,2] **and M. Guellal**[1]

Abstract: Combined laminar natural convection and surface radiation in a differentially heated square cavity has been investigated by a finite volume method through the concepts of staggered grid and SIMPLER approach. A power scheme has been also used in approximating advection–diffusion terms, determining the view factors by means of analytical expressions. The effect of emissivity on temperature and velocity profiles within the enclosure has been analyzed. In addition, results for local and average convective and radiative Nusselt numbers are presented and discussed for various conditions.

Keywords: Natural convection, surface radiation, Numerical simulation.

Nomenclature

A_i	radiative surface number i
A_{ij}	elements of matrix A
F_{i-j}	view-factor between the surfaces A_i and A_j
g	gravitational acceleration, $m.s^{-2}$
H	size of the enclosure, m
J_i	dimensionless radiosity of surface A_i
k	thermal conductivity, $W.m^{-1}.K^{-1}$
N	total number of radiative surfaces
Nr	radiation number, $\sigma T_0^4(k\Delta T/H)$
Nu	Nusselt number
p	fluid pressure , Pa
P	dimensionless pressure
Pr	Prandtl number, ν/α
q_r	net radiative flux, W.m^{-2}

[1] Laboratoire de Génie des Procédés Chimiques, Université de Sétif 1, Algeria.
[2] Faculté des Sciences et des Sciences Appliquées, Université de Bouira, Algeria. Corresponding author. Email: sa_hamimid@yahoo.fr

Q_r	dimensionless net radiative-flux
Ra	External Rayleigh number, $g\beta\Delta T H^3/(\nu\alpha)$
t	time, s
T	dimensional temperature, K
T_0	reference temperature, $(T_H + T_C)/2, K$
u, v	velocity components, $m.s^{-1}$
U, V	dimensionless velocity-components
x, y	cartesian coordinates , m
X, Y	dimensionless coordinates

Greek symbols

α	thermal diffusivity, m^2.s^{-1}
β	thermal expansion coefficient, K^{-1}
ΔT	temperature difference, $\Delta T = T_H - T_C$, K
ν	kinematic viscosity, $m^2.s^{-1}$
ρ	fluid density, $Kg.m^{-3}$
σ	Stefan–Boltzmann constant, W.m^{-1}.K^{-4}
θ	dimensionless temperature, $(T - T_0)/\Delta T$.
Θ	dimensionless radiative-temperature
δ_{ij}	Kronecker symbol
τ	dimensionless time

Subscripts

avg	average value
mid	midplan
0	reference state
C	cold
c	convective
H	hot
r	radiative
t	total

1 Introduction

Natural convection in rectangular cavities has received considerable attention in the literature due to its numerous applications of engineering interest [Mahmoudi (2013); Hamimid (2012); Rouijaa (2011)].

Combined natural convection and radiation exchange between surfaces involving a radiatively non-participating medium inside enclosures may appear in many practical situations of engineering interest, such as pane windows, solar collectors, building insulation, nuclear engineering, ovens and rooms. Although the surface radiation is inherent in natural convection, the interaction between the two phenomena has received a little attention.

The first numerical study of the coupled heat transfer problem involving both convection and radiation in a rectangular cavity seems to be that of Larson and Viskanta (1976). They found that radiation heats up very quickly both the cavity surface and gas body leading, hence, to a considerable modification of the flow pattern and the corresponding convection process.

A numerical study of combined laminar natural convection and surface radiation heat transfer in a modified cavity receiver of solar parabolic dish collector were presented by Reddy and Sendhil (2008). They observed that the convection and radiation heat losses are respectively 52% and 71.34% of the total heat loss at 0° inclination. These losses decrease to 40.72% and 59.28% at 90° inclination for the modified cavity receiver with an area ratio of 8 and 400°C.

Many studies on laminar and turbulent natural convection heat transfer including radiation were carried out [Balaji and Venkateshan (1994); Ramesh and Venkateshan (1999); Velusamy and Sundararajan (2001); Anil, K. Velusamy (2007); Alvarado and Xamán (2008); Xamán and Arce(2008); Dihmani (2012); Moufekkir (2012)]. Xamán et al. (2008) presented two-dimensional numerical study of combined heat transfer (laminar and turbulent natural convection, surface thermal radiation and conduction) in a square cavity with a glass wall. Their results showed that the flow pattern is not symmetric due to the combined effect of non-isothermal glass wall and radiative exchange inside the cavity.

In their investigation, Lauriat and Desrayaud (2006) numerically studied the heat transfer by natural convection and surface radiation in a two-dimensional vented enclosure in contact with a cold external environment and a hot internal one. They found that the radiative contributions to the heat transfer along the facing surfaces were the dominant heat transfer mode for all of the considered cases.

Recently, Amraqui et al. (2011) analyzed computation of the radiation–natural convection interactions in an inclined "T" form cavity. They concluded that the heat transfer decreases with increasing j (inclination angle). Moreover, they noted that the Rayleigh number increase number and the presence of radiation produce a considerable increase of the heat transfer.

Hinojosa et al. (2005) presented a numerical study of the heat transfer by natural convection and surface thermal radiation in a tilted 2D open cavity. They found that the convective Nusselt number changes substantially with the inclination angle of the cavity, while the radiative Nusselt number is insensitive to the orientation change of the cavity.

Ramesh and Merzkirch (2001) made an experimental study of the combined natural convection and thermal radiation heat transfer, in a cavity with top aperture; they found out that the surface thermal radiation heat transfer in cavities with walls of high emissivities has a significant change in the flow and temperature patterns and therefore influences the natural convection heat transfer coefficients.

Nouanegue et al. (2008), investigated conjugate heat transfer by natural convection, conduction and radiation in open cavities in which a uniform heat flux is applied to the inside surface of the solid wall facing the opening. They noticed that the surface radiation affects considerably the flow and temperature fields. The influence of the surface radiation is marked by the decrease of the heat fluxes due to natural convection and conduction while the heat flux by radiation increases with increasing surface emissivity. On the other hand, the convective and radiative Nusselt numbers are increasing with the surface emissivity for a given wall conductance. Both the combined Nusselt number and the volume flow rate are increase with the surface emissivity, particularly at high Rayleigh numbers. The convective and radiative Nusselt numbers are a decreasing function of the wall conductance and an increasing function of the aspect ratio. They noticed similar trends for the volume flow rate through the cavity.

The complete conjugate heat conduction, convection and radiation problem for a heated block in a differentially heated square enclosure is solved by Liu and Phan-Tien (1999). In comparison to the problem considered by House et al. (1990), the block generates heat. The conduction and the emission of the block have a substantial effect on the heat transfer situation.

In the present work, the two-dimensional unsteady simulation of the effects of radiation on natural convection flow in a square cavity whose four walls have the same emissivity is investigated. The surface emissivity ε, the Rayleigh number Ra and the radiation number Nr are parametrically varied.

2 Mathematical formulation

2.1 Governing equations

Details of the geometry are shown in Fig.1. The flow is assumed to be incompressible, laminar and two dimensional in a square cavity, the two horizontal end walls are perfectly insulated, while the two vertical walls are maintained at two different temperatures T_H and T_C, respectively ($T_H > T_C$). It will be further assumed that the temperature differences in the flow domain under consideration are small enough to justify the employment of the Boussinesq approximation.

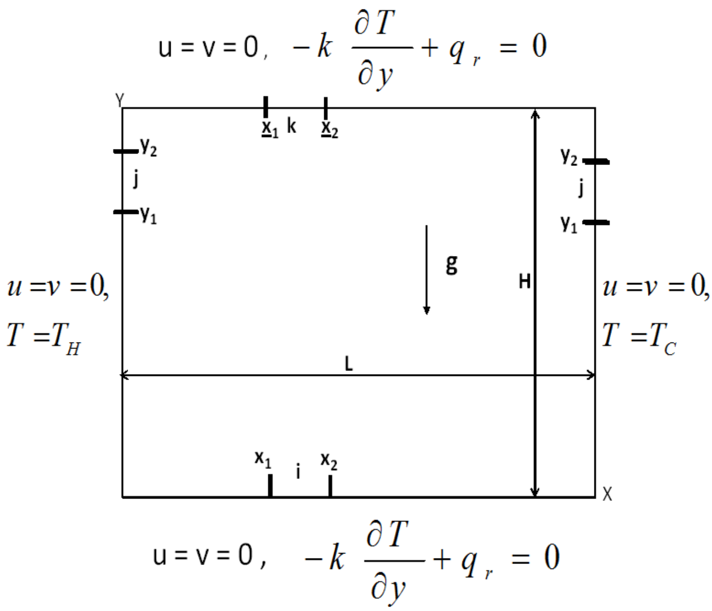

Figure 1: The flow configuration and coordinate system.

The fluid is the air and its properties are assumed constant at the average temperature T_0, except for the density whose variation with the temperature is allowed in the buoyancy term. The inner surfaces, in contact with the fluid, are assumed to be gray and diffuse, and could emit and reflect of radiation with identical emissivities.

The governing equations for this problem are based on the balance laws of mass, momentum and energy. Taking into account the assumptions mentioned above, the governing equations for the problem in two dimensions unsteady states can be written in dimensionless form as:

$$\frac{\partial U}{\partial X}+\frac{\partial V}{\partial Y}=0 \tag{1}$$

$$\frac{\partial U}{\partial \tau}+U\frac{\partial U}{\partial X}+V\frac{\partial U}{\partial Y}=-\frac{\partial P}{\partial X}+\mathrm{Pr}(\frac{\partial^2 U}{\partial X^2}+\frac{\partial^2 U}{\partial Y^2}) \tag{2}$$

$$\frac{\partial V}{\partial \tau}+U\frac{\partial V}{\partial X}+V\frac{\partial V}{\partial Y}=-\frac{\partial P}{\partial Y}+\mathrm{Pr}(\frac{\partial^2 V}{\partial X^2}+\frac{\partial^2 V}{\partial Y^2})+Ra\,\mathrm{Pr}\,\theta \tag{3}$$

$$\frac{\partial \theta}{\partial \tau}+U\frac{\partial \theta}{\partial X}+V\frac{\partial \theta}{\partial Y}=(\frac{\partial^2 \theta}{\partial X^2}+\frac{\partial^2 \theta}{\partial Y^2}) \tag{4}$$

The governing equations are non-dimensionalized using the following definitions of the dimensionless variables:

$$\tau = \frac{t}{H^2/\alpha}, \quad X = \frac{x}{H}, \quad Y = \frac{y}{H}, \quad U = \frac{uH}{\alpha}, \quad V = \frac{vH}{\alpha}, \quad P = \frac{pH^2}{\rho\alpha^2}, \quad \theta = \frac{T - T_0}{\Delta T}$$

2.2 Radiative analysis

The radiative surfaces of the solid forming the enclosure are divided into a set of zones (surfaces) A_i, i = 1,. . .N. N is the number of total radiative surfaces forming the cavity, which are equal to the total control volume solid–air interfaces. In fact, the control volume faces are also arranged so that a control volume face coincides with an interface solid–fluid.

The number of zones retained is determined by the mesh used to solve the differential equations. The grid is constructed such that the boundaries of physical domain coincided with the velocity grid lines.

Determination of the net radiative flux density requires the knowledge of the surface temperature of each node. The equation of the thermal balance of each surface provides us with these temperatures. Thus, one assumes that the solid surfaces are in thermal equilibrium under the combined action of the convective and radiative contributions, which gives:

$$-k\frac{\partial T}{\partial z} + q_r = 0 \tag{5}$$

z denotes the normal direction to the interface under consideration, and q_r is the net radiative flux density along this interface.

Eq. 5 is expressed in non-dimensional form as:

$$\left.\frac{\partial \theta}{\partial Y}\right|_{Y=0,1} - N_r Q_r|_{Y=0,1} = 0 \tag{6}$$

Where $Nr = \sigma T_0^4 H/k\Delta T$, is the dimensionless parameter of conduction-radiation and $Q_r = q_r/\sigma T_0^4$, is the dimensionless net radiative heat flux on the corresponding insulated wall.

Therefore, the dimensionless net radiative flux density along a diffuse-gray and opaque surface "A_i" is expressed as:

$$Q_{r,i} = J_i - \sum_{j=1}^{N} J_j F_{i-j} \tag{7}$$

J_i is the dimensionless radiosity of surface A_i , obtained by resolving the following system:

$$\sum_{j=1}^{N}(\delta_{ij}-(1-\varepsilon_i)F_{i-j})J_j=\varepsilon_i\Theta_i^4 \tag{8}$$

Where the dimensionless radiative-temperature Θ_i is given by:

$$\Theta_i=\frac{T_i}{T_0}=\frac{\theta_i}{\theta_0}+1 \tag{9}$$

The heat transfer problem is completed by initial and boundary conditions:

$$U=V=0,\quad \theta=\theta_i \quad for \quad \tau=0$$

$$U=V=0,\quad \theta=\theta_H=0.5 \quad for \quad 0\leq Y\leq 1 \quad at \quad X=0$$

$$U=V=0,\quad \theta=\theta_C=-0.5 \quad for \quad 0\leq Y\leq 1 \quad at \quad X=1$$

$$U=V=0,\quad \frac{\partial\theta}{\partial Y}-NrQ_r=0 \quad for \quad 0\leq X\leq 1 \quad at \quad Y=0$$

$$U=V=0,\quad \frac{\partial\theta}{\partial Y}-NrQ_r=0 \quad for \quad 0\leq X\leq 1 \quad at \quad Y=1$$

2.3 Heat transfer

The non-dimensional heat transfer rate in terms of convective and radiative Nusselt numbers, Nu_c and Nu_r, from the left vertical heated surface are given by:

$$Nu_c=-\left.\frac{\partial\theta}{\partial X}\right|_{Y=0} \tag{10}$$

$$Nu_r=N_rQ_r|_{Y=0} \tag{11}$$

The average convective Nusselt number is calculated integrating the temperature gradient over the heated wall as follows:

$$Nu_{c_{avg}}=\frac{1}{A}\int_0^A-\frac{\partial\theta}{\partial X}dX \tag{12}$$

The average radiative Nusselt number is obtained integrating the dimensionless net radiative flux over the heated wall, by the following mathematical relationship:

$$Nu_{r_{avg}}=N_r\frac{1}{A}\int_0^A Q_rdX \tag{13}$$

The total average Nusselt number is calculated by summing the average convective Nusselt number and the average radiative Nusselt number:

$$Nu_{avg}=\frac{1}{A}\int_0^A\left(-\left.\frac{\partial\theta}{\partial X}\right|_{0,Y}+N_rQ_r(0,Y)\right)dY \tag{14}$$

3 Numerical procedure

The numerical solution of the governing differential equations for the velocity, pressure and temperature fields is obtained by using a finite volume technique. A power scheme is also used in approximating advection–diffusion terms. The SIMPLER algorithm (Semi-Implicit Method for Pressure Linked Equations Revised) whose details can be found in Patankar (1980), with a staggered grid is employed to solve the coupling between pressure and velocity. The governing equations are casted in transient form and a fully implicit transient differencing scheme is employed as an iterative procedure to reach steady state. The discretised equations are solved using the line by line Thomas algorithm with two directional sweeps.

The radiosities of the elemental wall surfaces are expressed as a function of elemental wall surface temperature, emissivity and the shape factors. The radiosity (J_j) and temperature (T_i) are connected by a matrix of the type:

$$[A_{i,j}]\left\{J_j\right\} = \left\{\sigma T_i^4\right\} \tag{15}$$

The inverse of the matrix $[A_{i,j}]$ is determined (only once) by the Gauss elimination method. The coefficients of $[A]$ are constant and depend only on the emissivity and the shape factors have no dependence on the temperatures.

In 2D, the view factors formulations are analytic, [Howell, (1982)]:

$$F_{i-j} = \frac{-1}{2(x_2-x_1)}\left[\left.\sqrt{x_2^2+y^2}\right|_{y_1}^{y_2} - \left.\sqrt{x_2^2+y^2}\right|_{y_1}^{y_2}\right] \tag{16}$$

$$F_{i-k} = -\frac{1}{2(x_2-x_1)}\left[\left.\sqrt{(\underline{x}_2-x)^2+H^2}\right|_{x=x_1}^{x=x_2} - \left.\sqrt{(\underline{x}_1-x)^2+H^2}\right|_{x=x_1}^{x=x_2}\right] \tag{17}$$

A preliminary study is carried out to determine the optimum uniform grid (i.e. the best compromise between accuracy and computational costs). For the calculations reported in this study a 120 x 120 grid points is chosen to optimise the relation between the required accuracy and the computing time. However, increasing the number of grid points did not change the results appreciably. In order to obtain good convergence solutions, the convergence criterion for the residuals (in SIMPLER algorithm) was set at 10^{-5}.

The outer iterative loop (unsteady SIMPLER algorithm) is repeated until the steady state is achieved which occurs when the following convergences are simultaneously satisfied: $\left|\varphi_{ij}^{old}-\varphi_{ij}\right| \leq \varepsilon_\varphi$, where φ represents the variables U, V or θ.

Table 1: Nusselt number at active walls obtained with T_0 = 293.5 K and ΔT =10K . $Nu_t = Nu_c + Nu_r$; Comparison with values published by Wang et al. (2006).

Ra	H	ε	Wang et *al*. (2006)						Present work					
			Hot Wall			Cold Wall			Hot Wall			Cold Wall		
			Nu_c	Nu_r	Nu_t	Nu_c	Nu_r	Nu_t	Nu_c	Nu_r	Nu_t	Nu_c	Nu_r	Nu_t
10^4	0.021		2.246	0	2.246	2.246	0	2.246	2.246	0	2.246	2.246	0	2.246
10^4	0.021	0.2	2.260	0.507	2.767	2.268	0.499	2.767	2.262	0.507	2.769	2.271	0.498	2.769
10^4	0.021	0.8	2.249	2.401	4.650	2.278	2.372	4.650	2.255	2.401	4.656	2.284	2.371	4.656
10^5	0.045	0	4.540	0	4.540	4.540	0	4.540	4.532	0	4.532	4.532	0	4.532
10^5	0.045	0.2	4.394	1.090	5.484	4.411	1.073	5.484	4.398	1.090	5.489	4.417	1.072	5.489
10^5	0.045	0.8	4.189	5.196	9.385	4.247	5.137	9.384	4.200	5.196	9.397	4.261	5.136	9.397
10^6	0.097	0	8.852	0	8.852	8.852	0	8.852	8.863	0	8.863	8.863	0	8.863
10^6	0.097	0.2	8.381	2.355	10.736	8.417	2.319	10.736	8.379	2.355	10.734	8.416	2.318	10.734
10^6	0.097	0.8	7.815	11.265	19.080	7.930	11.150	19.078	7.861	11.265	19.126	7.971	11.151	19.126

4 Verification

In order to assess the accuracy of the numerical code, we present in Tab 1 the results representing convective, radiative and total Nusselt numbers at the active walls. An excellent agreement is found between the present computations and those obtained by Wang et *al*. (2006).

5 Results and discussion

In this investigation, both pure natural convection and natural convection coupled with surface radiation cases are presented. Each case required the specification of four dimensionless parameters ($0 \leq \varepsilon \leq 1, Ra = (10^4, 10^5, 10^6)$ corresponding *to* $H = (0.021, 0.045, 0.097)m$ and $Nr = (38.6, 83.13, 179.1)$ respectively; the other parameters such as Prandtl number, average temperature, temperature differences, and cavity aspect ratio are respectively held fixed to Pr = 0.70, T_0 = 300 K and ΔT=10K.

As soon as the walls emit, the surface radiation changes the temperature distribution along the adiabatic walls: the fluid is heated along the lower wall and cools along the upper wall. The convective Nusselt number along the hot wall decreases with increasing emissivity (Fig. 2). This decrease is more pronounced in the bottom portion of the cavity, unlike radiative and total Nusselt numbers, along the same wall, which increase with the emissivity increase (Fig.3, Fig.4).

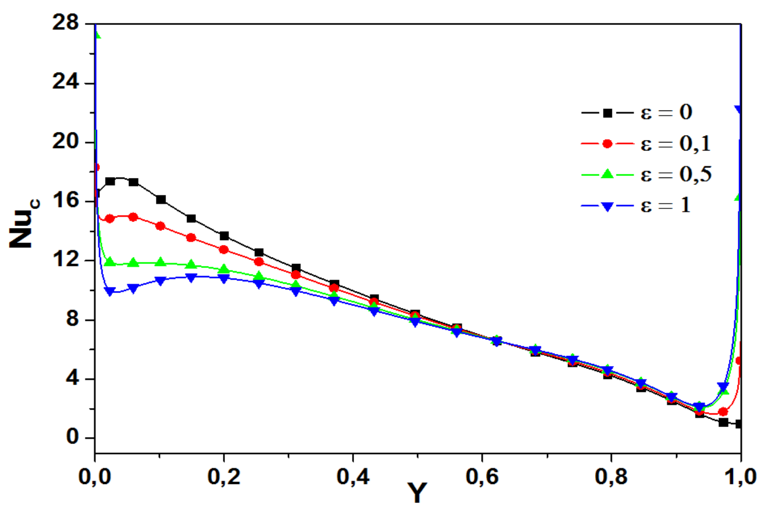

Figure 2: Distributions of the local Nusselt number on the heat wall for different ε and with *H=0.097 m*, $Ra = 10^6$.

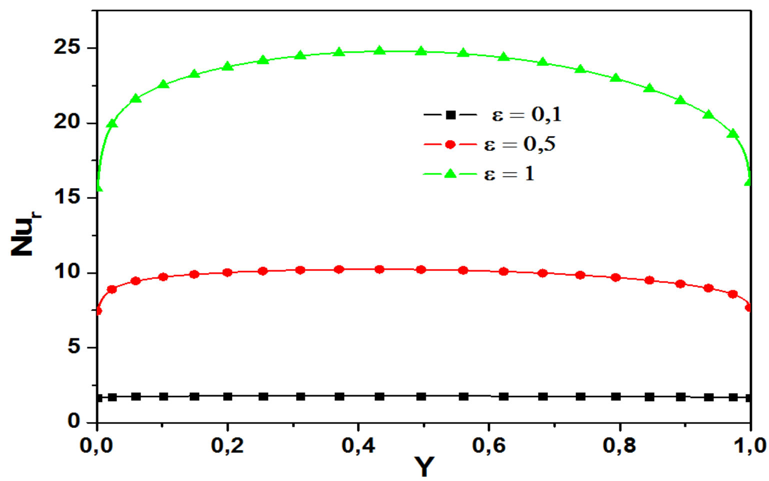

Figure 3: Distributions of the radiative Nusselt number on the heat wall for different ε and with *H=0.097 m*, $Ra = 10^6$.

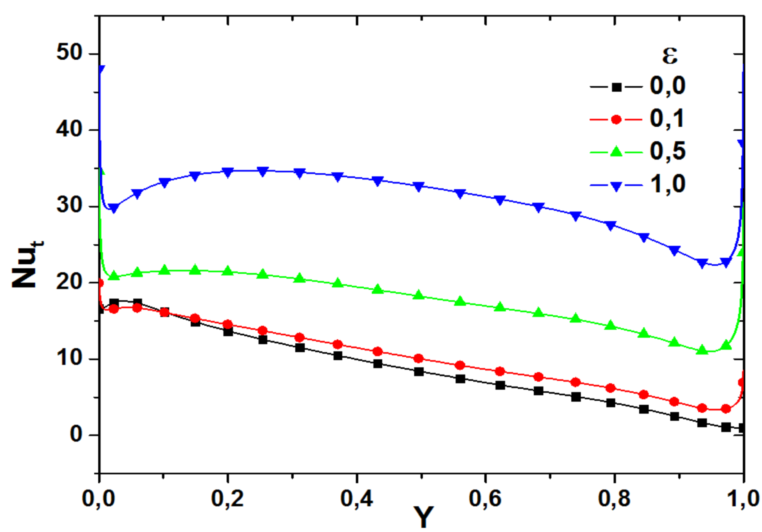

Figure 4: Distributions of the total Nusselt number on the heat wall for different ε and with *H=0.097 m*, $Ra = 10^6$.

Fig.6a and Fig.6b illustrate the influence of surface radiation on the fluid structure at Ra = 10^6. The effects are visible along the horizontal walls and at the center of the cavity. Compared to the case without radiation ($\varepsilon = 0$), air circulation is increased under radiation and isotherms structures near the walls are affected by thermal radiation. It appears from the isotherms that the radiation heat transfer produces a good homogenization of temperature especially in the cold part of the enclosure.The temperature gradients near the horizontal walls give an indication of the importance of the radiative flux. One can thus see that isotherms are inclined near adiabatic walls whereas they are perpendicular in the pure natural convection case, stratification is reduced in the center of the cavity, and thermal and dynamic horizontal boundary layers are strengthened (Fig.7). However, thermal and dynamic vertical boundary layers are not influenced by radiation (Fig.8).

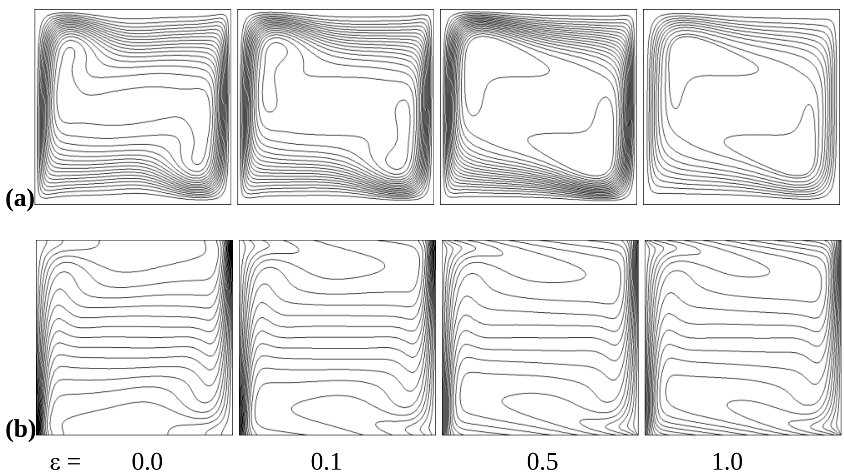

Figure 5: Streamlines **(a)** and isotherms **(b)** obtained for *Ra*=10^6, *H=0.097m,* T_0=300K , ΔT=10K, and various values of ε.

Fig. 9 shows the temperature distributions at the horizontal walls. We can see that the radiation exchange between the radiative surfaces increases the bottom wall temperature of the cavity, whereas the top wall temperature decreases. This reduction is the origin of the homogenization of the temperature inside the cavity.

Fig.10 shows the evolution of the average convective, radiative and total Nusselt numbers for different values of the emissivity ε and for different Rayleigh number *Ra*. One can notice that the average convective Nusselt number Nu_c decreases with increasing the emissivityε. This seems obvious since the dimensionless net radiative flux Q_r along the hot wall and consequently Nu_r are proportional to ε.

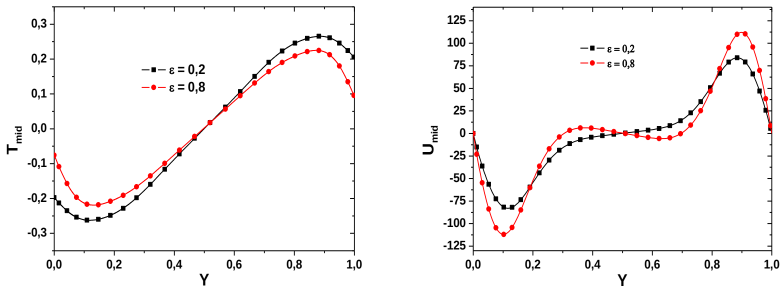

(a) (b)

Figure 6: Temperature (a) and horizontal velocity (b) profiles at *x*= 0.5 for *Ra* = 10^6 and *H=0.097 m*.

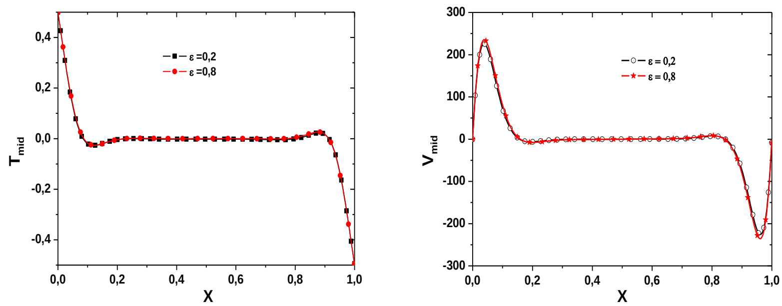

(a) (b)

Figure 7: Temperature (a) and vertical velocity (b) profiles at y = 0.5 for *Ra*= 10^6 and *H=0.097 m*.

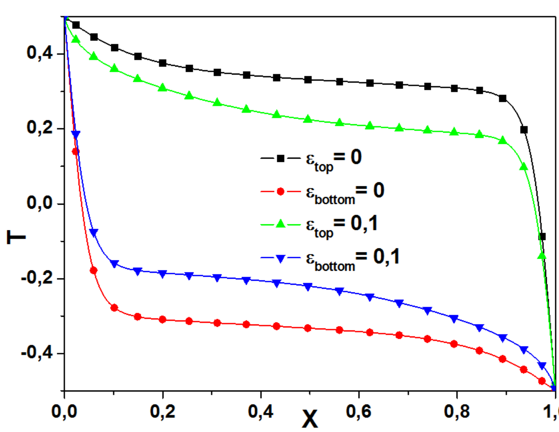

Figure 8: Temperature distributions on the horizontal walls at Ra=10^6 and *H=0.097 m*.

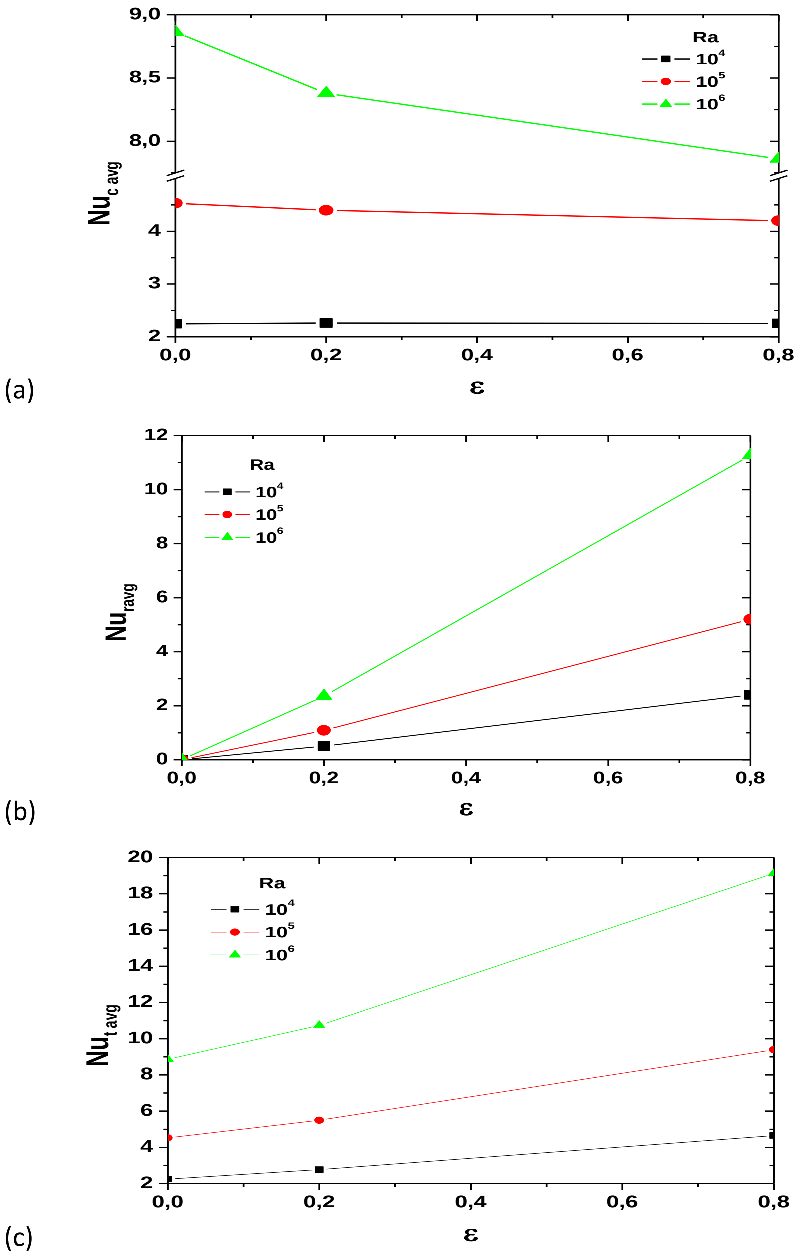

Figure 9: Variations of the average convection (a), radiation (b) and total (c) Nusselt number as a function of emissivity ε, for $\Delta T = 10k$, *H=0.021, 0.045, 0.097 m* and various Rayleigh number.

6 Conclusion

In the present paper, calculations have been made for the combined natural convection and radiation in a differentially-heated cavity. Within the investigated parameter ranges, the numerical study shows that the thermal radiation affects the isotherms near solid adiabatic surfaces, since the inclination of the isotherms indicates the importance of the thermal radiation heat transfer. It is also noted that the thermal radiation increases the flow velocity inside the cavity. We concluded that the surface radiation modifies the flow and temperature fields. The modification starts at low surface emissivity and increases gradually with it. On the other hand, the convective and radiative Nusselt numbers respectively decrease and increase with the surface emissivity.

References

Alvarado, R.; Xamán, J.; Hinojosa, J.; Álvarez, G. (2008): Interaction between natural convection and surface thermal radiation in tilted slender cavities. *Int. J. Thermal Sciences,* vol. 47, pp. 355-368.

Amraqui, S.; Mezrhab, A.; Abid, C. (2011): Computation of coupled surface radiation and natural convection in an inclined "T" form cavity. *Energy Conversion and Management,* vol. 52, pp. 1166-1174.

Anil, K. S.; Velusamy, K.; Balaji, C.; Venkateshan, S. P. (2007) : Conjugate turbulent natural convection with surface radiation in air filled rectangular enclosures. *Int. J. Heat Mass Transfer*, vol. 50, pp. 625-639.

Balaji, C.; Venkateshan, S. P. (1994) : Combined surface radiation and free convection in cavities. *J. Thermophys. Heat Transfer,* vol. 8, pp. 373-376.

Dihmani, N.; Amraqui, S.; Mezrhab, A; Laraqi, N. (2012): Numerical Modelling of Rib Width and Surface Radiation Effect on Natural Convection in a Vertical Vented and Divided Channel. *Fluid Dyn. Mater. Process,* vol. 8 no.3, pp. 311-322.

Hamimid, S.; Guellal, M; Amroune, A.; Zeraibi, N. (2012): Effect of a Porous Layer on the Flow Structure and Heat Transfer in a Square Cavity, *Fluid Dyn. Mater. Process*, vol.8, no.1, pp. 69-90

Hinojosa, J. F.; Cabanillas, R. E.; Alvarez, G.; Estrada, C. E. (2005) : Nusselt number for the natural convection and surface thermal radiation in a square tilted open cavity. *International Communications in Heat and Mass Transfer*. vol. 32, pp. 1184-1192

Hong Wang; Shihe Xin; Patrick Le Quéré, (2006) : Étude numérique du couplage de la convection naturelle avec le rayonnement de surfaces en cavité carrée remplie d'air. *C. R. Mecanique*, vol. 334, pp. 48-57

House, J. M.; Beckermann, C.; Smith, T. F. (1990): Effect of a centered conducting body on natural convection heat transfer in an enclosure. *Num. Heat Transfer,* vol. 18, pp. 213-225.

Howell, J. R. (1982): *A Catalog of Radiation Configuration Factors*, McGraw-Hill.

Larson, D. W.; Viskanta, R. (1976): Transient combined laminar free convection and radiation in a rectangular enclosure. *J. Fluid Mech,* vol. 78, pp. 65-85.

Lauriat, G.; Desrayaud, G. (2006): Effect of surface radiation on conjugate natural convection in partially open enclosures. *Int. Journal of Thermal Sciences,* vol. 45, pp.335-346.

Liu, Y.; Thien, N. P. (1999): A complete conjugate conduction convection and radiation problem for a heated block in a vertical differentially heated square enclosure. *Comput. Mech.* vol. 24, pp. 175-186.

Mahmoudi, A.; Mejri, I.; Abbassi, M. A.; Omri, A. (2013): Numerical Study of Natural Convection in an Inclined Triangular Cavity for Different Thermal Boundary Conditions: Application of the Lattice Boltzmann Method. *Fluid Dyn. Mater. Process,* vol. 9, no.4, pp. 353-388.

Moufekkir, F.; Moussaoui, M. A.; Mezrhab, A.; Naji, H.; Bouzidi, M. (2012): Numerical Study of Double Diffusive Convection in presence of Radiating Gas in a Square Cavity. *Fluid Dyn. Mater. Process,* vol. 8, no. 2, pp. 129-154.

Nouanegue, H.; Muftuoglu, A.; Bilgen, E. (2008): Conjugate heat transfer by natural convection, conduction and radiation in open cavities. *International Journal of Heat and Mass Transfer,* vol. 51, pp. 6054-6062.

Patankar, S. V. (1982): Numerical heat transfer and fluid flow. McGraw-Hill

Ramesh, N.; Merzkirch, W. (2001): Combined convective and radiative heat transfer in side-vented open cavities. *Int. J. Heat Fluid Flow* . vol. 22, no. 2, pp. 180–187.

Ramesh, N.; Venkateshan, S. P. (1999): Effect of surface radiation on natural convection in a square enclosure. *J. Thermophys. Heat Transfer,* vol. 13, pp. 299-301.

Reddy, K. S.; Sendhil Kumar, N. (2008): Combined laminar natural convection and surface radiation heat transfer in a modified cavity receiver of solar parabolic dish. *International Journal of Thermal Sciences,* vol. 47, pp.1647-1657.

Rouijaa, H.; El Alami, M.; Semma, E.; Najam, M. (2011): Natural Convection in an Inclined T-Shaped Cavity. *Fluid Dyn. Mater. Process*, vol. 7, no. 1, pp. 57-70.

Velusamy, K.; Sundararajan, T.; Seetharamu, K. (2001) : Interaction effects between surface radiation and turbulent natural convection in square and rectangular enclosures. *J. Heat Transfer,* vol. 123. pp. 1062-1070.

Xamán, J.; Arce, J.; Álvarez, G.; Chávez, Y. (2008): Laminar and turbulent natural convection combined with surface thermal radiation in a square cavity with a glass wall. *International Journal of Thermal Sciences,* vol. 47, pp. 1630-1638.